A New Technique for Digital Fluoroscopic Video Assessment of Sagittal Plane Lumbar Spine Motion

Article *in* Spine · August 2005

DOI: 10.1097/01.brs.0000170589.47555.c6 · Source: PubMed

4 authors, including:

Timothy William Flynn
South College
110 PUBLICATIONS **3,530** CITATIONS
SEE PROFILE

Lawrence Abraham
University of Texas at Austin
59 PUBLICATIONS **1,708** CITATIONS
SEE PROFILE

SPINE Volume 30, Number 14, pp E406–E413

A New Technique for Digital Fluoroscopic Video Assessment of Sagittal Plane Lumbar Spine Motion

Deydre S. Teyhen, PT, PhD, OCS,*†‡ Timothy W. Flynn, PT, PhD, OCS, FAAOMPT,§ Alan C. Bovik, PhD,¶ and Lawrence D. Abraham, EdD†

Study Design. Methodological reliability.

Objective. Develop a measurement technique to assess dynamic motion of the lumbar spine using enhanced digital fluoroscopic video (DFV) and a distortion compensated roentgen analysis (DCRA).

Summary of Background Data. Controversy over both the definition and consequences of lumbar segmental instability persists. Information from static imaging has had limited success in providing an understanding of this disorder. DFV has the potential to provide further information about lumbar segmental instability; however, the image quality is poor and clinical application is limited.

Methods. DFV from 20 male subjects (11 with and nine without low back pain) were obtained during eccentric lumbar flexion (30 Hz). Each DFVs was enhanced with a series of filters to accentuate the vertebral edges. An adapted DCRA algorithm was applied to determine segmental angular and linear displacement. Both intraimage and interimage reliability were assessed using intraclass correlation coefficients (ICC) and standard error of the measurement (SEM).

Results. Intraimage reliability yielded an average ICC of 0.986, and the SEM ranged from 0.4–0.7° and 0.2–0.3 mm. Interimage reliability yielded an average ICC of 0.878, and the SEM ranged from 0.7–1.4° and 0.4–0.7 mm.

Conclusions. Enhanced DFV combined with a DCRA resulted in reliable assessment of lumbar spine kinematics. The error values associated with this technique were low and were comparable to published error measurements obtained when using a similar algorithm on hand-drawn outlines from static radiographs.

Key words: biomechanics, kinematics, fluoroscopy, lumbar spine. **Spine 2005;30:E406–E413**

Despite the exponential rise in surgical rates of lumbar spinal fusion and the dedication of medical resources for recurrent surgical procedures[1–3] there remains no clear consensus on what constitutes lumbar segmental instability (LSI) or how LSI is related to low back pain (LBP). The clinical diagnosis of LSI is still largely based on patient history and certain inconclusive findings.[4] Improved knowledge of spinal kinematics may allow for better selection of surgical candidates and treatments, which would improve the surgical success rates while decreasing the medical costs associated with chronic LBP. However, to date, no definitive relationship exists between intervertebral motion and the clinical symptoms attributed to LSI. This is in part because of a lack of a noninvasive measurement tool to assess lumbar kinematics.

Radiographic assessment of lumbar motion has traditionally relied on static end-range radiographic measurements, in which measurements of hypermobility in flexion and extension have been used to define those with LSI.[5] However, many problems have existed with traditional radiographic assessments for LSI. Variability of normal human movement in asymptomatic individuals,[5–11] age and time with a lumbar disorder,[12–14] level of pain,[9,15,16] normal and abnormal coupled movement of the functional spinal units during motion,[7,17,18] and differences in test postures used to analyze the motion[6,19–23] have limited the usefulness of measures of hypermobility to denote instability. Furthermore, traditional imaging techniques have been assessed statically at end-range motion,[5–7,10,17,20,24,25] which has been found to be inadequate to categorize these patients.[3,19,23,26,27] Finally, traditional measurement techniques have been associated with large measurement error.[15,25,28–31] Techniques that decrease this error and that improve the ability to standardize the measurement technique, which include proper landmark verification techniques, have been suggested to measure intersegmental motion successfully.[21,32–42]

A landmark verification protocol developed by Brinckmann *et al*[41] was designed to limit errors by compensating for radiographic distortion of the central beam, off-center position, axial rotation, and lateral tilt during the objective determination of the vertebral corner locations. A follow-on study by Frobin *et al*[39] enhanced this protocol by developing an intersegmental measuring technique to assess intersegmental angular and linear displacement in the sagittal plane using geometric parameters that are symmetric with respect to the adjacent vertebral bodies. Although this measurement technique has the least amount of reported error for a noninvasive technique,[38] it has only been applied to digitized hand-drawn outlines of vertebral bodies from static images.

From the *U.S. Army-Baylor University Doctoral Program in Physical Therapy, Fort Sam Houston, Houston, Texas; the † Movement Science Program, Department of Kinesiology and Health Education, and the ¶Laboratory for Image and Video Engineering, Department of Electrical and Computer Engineering, University of Texas in Austin, Austin, Texas; the ‡Spine Research Center, Department of Orthopaedics, Walter Reed Army Medical Center, Washington DC; and the §Department of Physical Therapy, Regis University, Denver, Colorado

Acknowledgment date: November 2, 2004. Acceptance date: December 6, 2004.

The manuscript submitted does not contain information about medical device(s)/drug(s).

No funds were received in support of this work. No benefits in any form have been or will be received from a commercial party related directly or indirectly to the subject of this manuscript.

Address correspondence and requests for reprints to Deydre Teyhen, U.S. Army-Baylor University Doctoral Program in Physical Therapy, 3151 Scott Road, Room 1303, Fort Sam Houston, TX 78234; E-mail: dteyhen@satx.rr.com

Table 1. Subject Demographics

	LBP (n = 11)	Control (n = 9)
Age (yrs)	36.4 ± 7.2 (24–45)	30.4 ± 8.0 (19–44)
BMI (kg/m^2)	28.4 ± 2.3 (23.8–32.3)	25.5 ± 3.4 (21.7–31.4)
Waist:Hip Ratio	0.917 ± .038 (0.872–1.004)	0.854 ± 0.062 (0.797–0.985)

Note. Values are mean ± SD, with range shown in parentheses.

Table 2. Test Administration

Outline	Procedures
Orientation	Completed questionnaires
	Screened for inclusion and exclusion criteria
	Provided informed consent
	Wore loose fitting clothes
Pre-DFV collection	Walked 5 minutes
	Removed shirt
	Placed in lower extremity stabilizing device
	Calibration images
	Instruction of movement pattern
	Two practice trials
DFV collection	Subjects performed a total of 4 movements, the 3rd movement was captured for analysis
	2 minute rest and 2 minutes of walking
	Replaced in stabilizing device
	Second image captured

Digital fluoroscopic video (DFV) has been suggested as a possible tool for analysis of lumbar motion based on the ability to observe the motion occurring during a dynamic range.[43–47] If these observations could be quantitatively assessed so that kinematic variables of the lumbar spine are reliably produced, they might provide a better understanding of normal and abnormal lumbar movement, which may lead to a new assessment tool to help define this population. However, poor image quality has limited its role. Application of image processing techniques to improve the distinction between vertebral bodies and the surrounding soft tissue may provide an opportunity to use DFV to quantify vertebral motion. To date, this approach has not been routinely used for the lumbar spine. Therefore, the purpose of this study was to develop a reliable measurement technique that would allow for the assessment of sagittal plane lumbar spine (L3-S1) kinematics using enhanced DFV and an adapted distortion compensated roentgen analysis (DCRA) technique.

■ Materials and Methods

Study Participants. A convenience sample of 20 male volunteers (Table 1) from the Department of Defense beneficiary population was recruited for this study. Eleven of the men were diagnosed with mechanical low back pain (MLBP) and were required either to be seeking care, to have limited their work activities, or to have limited their recreational activities secondary to MLBP of subacute or chronic nature. Their history of MLBP varied from 1 month to 20 years of symptoms, with all volunteers complaining of a minimum of one prior episode of MLBP before the current episode. The modified Oswestry Disability Index (ODI) score for the group was 30.4 ± 8% (19–44%). Minimal inclusion and exclusion criteria were placed on this group in order to obtain a variety of possible different movement dysfunctions to include both hypo- and hypermobile individuals. However, individuals with acute pain that restricted sagittal plane motion, neurologic changes in strength, or a history of spinal surgery were excluded from this study.

Nine volunteers were defined as not having LBP. Screening criteria adapted from Hayes *et al*[10] and an ODI score ≤4% were used to screen for a lack of LBP over the last 3 years. Of these nine individuals, only two had a history of an episode of MLBP in high school (10 and 24 years ago) and only one volunteer had a positive ODI score (4%). Females were not included in this study because of increased radiation exposure to the reproductive organs.

The research protocol was approved by the Institutional Review Boards at the University of Texas in Austin and at Brooke Army Medical Center. A radiation safety review was conducted by the radiation health physicist at the medical center. All volunteers provided their informed consent and signed a health insurance portability & accountability act form.

Instrumentation. DFV was collected with a Philips Radiographic/Fluoroscopy Diagnost 76 system (Philips Medical Systems, Andover, MA) in its upright position. The images were digitized by an I-75 frame grabber (Foresight Imaging, Lowell, MA)[48] that was reported to capture the images at 8 bits per pixel with ±1 nanoseconds pixel jitter.[48] The I-75 frame grabber has a reported pixel rate of 75 MHz[48] and captured the DFV at 30 Hz. The images were stored and processed on a personal computer. Image Pro-Plus (MediaCybernetics, Silver Springs, MD),[49] MATLAB (The Math Works, Natick, MA),[50] Microsoft Excel (Microsoft Computer Corp., Redmond, WA), and SPSS 11.0 (SPSS Inc. Chicago, IL)[51] were used for analysis.

Collection of DFV. Test procedures used in the collection of the DFV are outlined in Table 2. Calibration images were obtained to ensure that the L3-S1 region was maintained within the field of view during the test movement, to calibrate the pixel width, and to adjust the kilovolts peak to optimize image quality. The average pixel per millimeter value from two images obtained with a radio-opaque ruler representing the near and far side of the subject's trunk was used to calibrate the DFV for the plane of the spine. Further, to improve the quality of the image and to prevent "white-out" during flexion, a lead harness was placed on the back of each subject.

DFV was obtained during sagittal plane flexion and extension. Subjects started in an upright posture, with the hands behind the head and the elbows pointing up towards the ceiling. The flexion and extension motion consisted of the subject slowly bending forward and returning to upright in approximately 4–5 seconds. Hyperextension (extension beyond the upright posture) was not tested in this study. Sagittal plane motion was selected not only because it is a movement associated with symptoms in those with LSI, but sagittal plane motion has greater ROM and is associated with only minimal out-of-plane motion as compared with frontal plane motion.[52–54] To further minimize out-of plane motion and to minimize ankle, knee, and hip motion, subjects were placed in a lower extremity stabilizing device[43] with the right side of the body next to the upright table (Figure 1). During pilot testing, this device was found to be essential to maintain the area of interest within the field of view while not restricting lumbar motion.

Figure 1. This figure demonstrates a subject in the upright posture in the stabilizing device. The stabilizing device consists of a rock-climbing harness with four nylon straps. Two straps are placed through the rock-climbing harness to the metal railing posterior to the subject to minimize hip and pelvic movement. The two straps around the knee are to minimize knee flexion.

Immediately after the practice trials, the subjects performed four cycles of flexion and extension, with the third cycle being captured by the fluoroscopic system, to ensure motion was captured throughout a full cycle. The subjects were then removed from the stabilizing device and rested for 2 minutes followed by 2 minutes of walking. Following the break, the subjects were repositioned in the stabilizing device and were reimaged for test-retest reliability (interimage reliability).

DFV Analysis. DFV analysis consisted of three separate steps: image processing, vertebral body detection, and kinematic analysis. During the image processing step, the vertebral bodies of the DFV were enhanced so that the edges became more defined. Vertebral body detection consisted of determining the corner and midpoint locations of the vertebral bodies. The third step, kinematic analysis of the motion, was used to determine global and segmental motion during the test movement.

The original DFV (Figure 2A) was processed with a combination of four image processing techniques to enhance the borders of the vertebral bodies from the surrounding soft tissue.[55,56] First, a large aperture band-pass filter was applied to the DFV (Figure 2B) to remove high frequency noise, enhancing image sharpness and contrast while also enhancing the edges of the vertebral bodies. Specifically, a 5×5 window was applied for the low-pass portion of the filter, followed by a 71×71 window for the high-pass portion of the filter. During pilot testing of different filter parameter conditions viewed by two orthopaedic spine surgeons, this filter (Figure 2A) achieved the clearest DFV visualizations.

Next a large aperture (50×50 window) edge detection filter was applied to the DFV (Figure 2C). This filter was designed to enhance the dark features of an image (the vertebral bodies) on a brighter background. A median filter (7×7 window) was then applied to the DFV (Figure 2D) to decrease impulse noise, which effectively enhanced the edges of the vertebral bodies. Finally, the results of the median filtered DFV were subtracted from the results of the band-passed DFV to create a DFV in which most of the edges of the vertebral body appeared as black (Figure 2E). The techniques described were robust and resulted in improved image quality for all subjects regardless of stature and without adjustment across subjects.

Other image processing techniques were attempted before adopting the technique described above. To determine the optimal image processing technique a point placement study was conducted on five different image processing techniques. It consisted of the selection of 10 vertebral corner locations on five different frames, representing different angles of lumbar flexion; each was measured five times (250 points per image processing technique). The average difference from mean pixel location for the technique described above was 1.86 ± 1.63 pixels, whereas placement error for the other four techniques ranged from 2.28 ± 1.19 to 2.60 ± 1.27 pixels. Therefore, the technique described resulted in the least amount of variability in corner selection by the rater.

After the DFV was processed, the next step was to locate the vertebral corner and midpoint locations. The technique used was based on the work of Frobin *et al*[39,40] and Brinckmann *et al*.[41] Vertebral corner locations (numbered 1–4; Figure 3) were

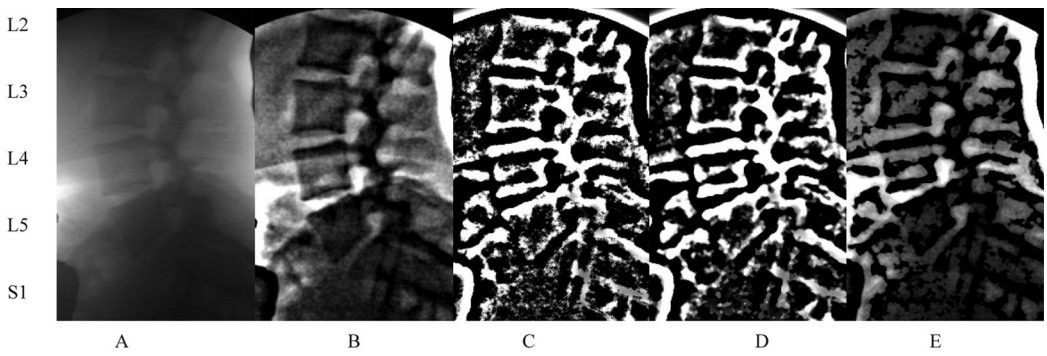

Figure 2. **A,** The original unprocessed image; **B,** Band-passed image; **C,** Edge detection image; **D,** Median filter image; **E,** Subtraction (**B-D**) image.

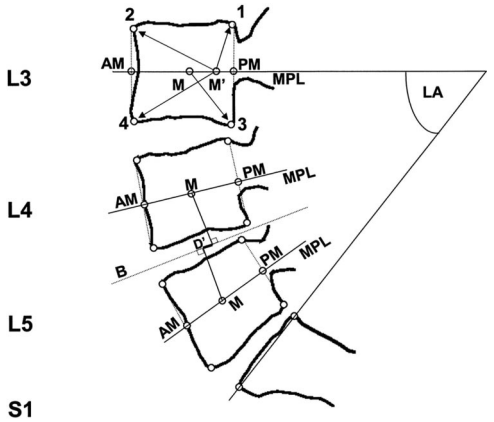

Figure 3. Vertebral body detection and kinematic analysis based on the work by Frobin *et al*[40] and Saraste *et al*.[21] The locations of the vertebral corners (numbered 1–4) are demonstrated on the L3 vertebral body. The anterior (AM), posterior (PM), and vertebral body (M & M′) midpoint locations are also demonstrated. The algorithm to find the vertebral corner locations was based on the maximum distance from the appropriate midpoint location, as demonstrated by the arrows drawn on L3. The intervertebral angle was defined as the angle between adjacent midplane lines (MPL). The first step to determine intersegmental displacement was to calculate the distance (D′) between the perpendicular projections of adjacent vertebral body center points to the bisectrix (B) between adjacent vertebral bodies (demonstrated on L4–L5). Linear displacement was then determined by dividing (D′) by the mean depth of the cephalad vertebral body to normalize the results and to compensate for distortion. Anterior (positive) migration occurred if the cephalad vertebral body's projection to the bisectrix was anterior to the caudal vertebral body's projection. Posterior (negative) displacement was defined when the reverse occurred. L3-S1 lordosis angle (LA) was defined as the angle between the MPL of L3 and the cephalad border of S1.

first estimated manually by the researcher. After the vertebral body midpoint (M) and 60% posteriorly displaced midpoint (M′) locations were calculated (Figure 3), a maximum distance formula was used to determine the objective vertebral corner locations based on the appropriate midpoint.[41] Specifically, the locations of the objective vertebral corners for L3-L5 were determined based on finding the lowest gray-scale value furthest from the appropriate midpoint location based on a 7×7 pixel width window placed centrally at the current estimated corner location. Three iterations of the computer-algorithm were processed to determine the best estimates of the vertebral corner and midpoint locations. The use of four iterations (one from the researcher and three computer assisted) of the vertebral corner selection process was in agreement with the work by Cholewicki *et al*[57] to minimize error. The location of the first sacral body was determined by its cephalad corners, the midpoint of that line was determined, and the maximal distance algorithm was applied as described above. Once the four estimates of the vertebral corner and midpoint locations were calculated, they were averaged to determine the final locations for that video frame.

Unlike the protocol described by Frobin *et al*[39,40] and Brinckmann *et al*[41] in which the hand-drawn outlines of the vertebral bodies were digitized, these DFV images included adjacent bone and soft tissue that would sometimes interfere with the vertebral corner location algorithm. Therefore, the goal of this algorithm was to ensure a large enough window size to search for the best estimate of the vertebral corner locations, while minimizing the chance of adjacent tissue being labeled inappropriately. Three window sizes were tested: 5×5, 7×7, and 9×9, which would allow the corner locations to vary by 6, 9, and 12 pixels (there were approximately 4 pixels per millimeter), respectively, through the algorithm iterations. The initial window size (5×5) was chosen as a starting point based on the point placement error study described previously. A pilot study of 3836 vertebral corner points found that only 1.3% (14 of 1,096) and 0.5% (5 of 1,096) of the midpoint locations changed when the window size was increased from 5×5 to 7×7, and 7×7 to 9×9, respectively. Therefore, a 7×7 window was determined to allow for exploration of the best-estimate of a vertebral corner location, while minimizing the possibility of adjacent soft tissue influencing the determination of vertebral corner position.

Once the "best-estimates" of the vertebral corners and midpoints locations were obtained for each frame, the estimates were smoothed across the frames to minimize the effect of small contour irregularities and variations in the digital image during the motion pattern and to minimize the effects of the image processing technique on the vertebral body contours. This was accomplished by a fourth order Butterworth filter with a 1.5 Hz cut-off frequency. These final midpoint locations of each vertebral body and the anterior and posterior vertebral body midpoint locations were used to determine the lumbar spine kinematic variables.

Although this protocol was based on the work of Frobin *et al*[39,40] and Brinckmann *et al*,[41] there are some distinct differences. First, the image processing technique described above allows for the algorithm to be applied directly to the DFV, while Frobin *et al*[39,40] and Brinckmann *et al*[41] relied on digitization of manual drawings of the vertebral body outlines. A second difference was the detection of the first sacral body (S1) position and orientation. This technique only determined the cephalad border of the sacrum, because it was not possible to visualize routinely the caudal border of the first sacral body with DFV. Further, this adjustment allowed for the maximum distance formula to be applied to both cephalad corner locations of S1, un-like the original algorithm in which only one of the four corner locations was able to be processed through the algorithm described. Diagrammatic movies of final vertebral body corner and midpoint locations were created as a quality control measure to ensure that the final data points represented the vertebral movement observed on the DFV.

On the basis of the location and orientation of the anterior, posterior, and vertebral body midpoints, global and segmental motion were determined. The global angle of L3-S1 lordosis was determined based on the review by Saraste *et al*[21] (Figure 3). Lordosis (L3-S1) was determined as the angle between the midplane line of L3 and the cephalad border of S1. Local extremes of lordosis angle were used to determine the upright and flexed postures. Intersegmental motion (angle and displacement) was calculated as described by Frobin *et al*[40] (Figure 3). The use of a bisectrix divided by the mean depth of the cephalad vertebral body to measure displacement and the use of midpoint locations to determine these kinematic variables were in agreement with suggestions by Muggleton and Allen[52] and by Harvey *et al*[53] to minimize the effects of distortion, orientation, out-of-plane motions, and point placement errors.

Reliability Procedures. Intraimage reliability was tested to analyze the reliability of the point-placement technique and the computer algorithm from repeated measures of the same set of

Table 3. Intraimage ICC and SEM for the Current Study and Comparison with Frobin *et al*[40]

	Current Study			Frobin et al[40]	
Segment	n*	ICC (2,12)	SEM (95% CI)	n †	SD (95% CI)
Midplane angle range (degrees)					
L3–L4	40	0.988	0.40° (0.81°)	54	0.85° (1.7°)
L4–L5	40	0.966	0.72° (1.44°)	52	1.32° (2.64°)
L5-S1	40	0.993	0.58° (1.17°)	11	1.64° (3.28°)
Average		0.982	0.57° (1.14°)		
Intersegmental displacement range (mm) ‡					
L3–L4	40	0.988	0.20 mm (0.40 mm)	54	0.52 mm (1.04 mm)
L4–L5	40	0.981	0.31 mm (0.63 mm)	52	0.55 mm (1.10 mm)
L5-S1	40	0.989	0.27 mm (0.54 mm)	11	0.84 mm (1.68 mm)
Average		0.986	0.26 mm (0.52 mm)		

* n = 40 images from 20 subjects (flexion and upright).
† For L3–L4 and L4–L5: 6 cadaver specimens, 9 radiographs taken in different (0, +5, −5) degrees of rotation or tilt, for L5-S1:11 images of a bony phantom taken at different distances from the image intensifier.
‡ Example for intersegmental displacement was based on a vertebral depth of 35 mm (i.e., 0.2/35 mm = 0.005711 or 0.57% relative displacement)

images. Repeated measures of 20 subjects were analyzed in the upright and flexed postures (three repetitions of 40 single images, a total of 240 analyzed images, or a total of 3360 individually placed points). The subject order was randomized by a second party and the randomized order varied between each measurement trial. By analyzing alternating upright and flexed images, recall bias on the vertebral corner point placement locations was minimized. The use of only single upright and flexed images, instead of continuous data, prevented use of smoothing and so the average of three repetitions were used to represent each image. The average intersegmental midplane angle and displacement values and L3-S1 lordosis (Figure 3) were calculated in each posture. Interimage reliability assessed the reliability of data obtained from two separate movement trials, separated by a 2-minute rest and 2-minute walk break. This design allowed the assessment of the additional error expected associated with subject repositioning and the variation of human movement between trials, while minimizing threats to internal validity (history and maturation) associated with repeated measures on separate occasions by having the subject tested on the same day. To minimize rater bias the analysis of the first and second movement trials by the rater were separated by a minimum of 2 months. Each DFV was analyzed from the upright position through the end-range flexion. The average time required for this motion was 2.27 ± 0.67 seconds, resulting in an average of 68 ± 20 frames per motion sequence, or 952 ± 280 point placements per motion sequence, for a total of 2,739 frames or 38,346 point placements. To assess the intersegmental motion based on a common global motion pattern, each set of DFV images for a subject was standardized to a common lordosis angle for both the upright and flexed postures. The standardized upright posture was the minimum lordotic angle of agreement in the upright postures, whereas the standardized flexed posture was the maximum lordotic angle of agreement in the flexed postures.

Statistical Analyses. An intraclass correlation coefficients (ICC), model (2, *k*), was calculated to determine a reliability coefficient. Model two was chosen because it acknowledges the role of the computer algorithm in determining the kinematic variables, it was designed to allow greater generalizability than model three, and it was more conservative than model three.[58] The kinematic variables were calculated based on averaged measurements; therefore, the averaged version of the ICC was calculated (*k*). In the analysis of intraimage reliability, $k = 12$, because each image was a mean of three cycles of the algorithm, each representing the mean of four anatomic landmark locations. In the analysis of interimage reliability, $k = 4$ to represent a single cycle of the algorithm for each movement analyzed. The standard error of the measurement (SEM) was calculated to determine the response stability of each measure.[58] In addition to the reliability measures calculated, the mean difference and the SD of the point placements of the intraimage analysis were calculated to compare the alteration of the DCRA technique with the original protocol.[40]

■ Results

Intraimage Reliability. The analysis of the rater's point placement technique revealed a mean difference in the displacement ratio of the paired measurements across segments for displacement of 0.05 ± 1.48% of the vertebral body depth, while the mean difference of the paired measurements across segments for midplane angle was 0.015 ± 0.992°. The intraimage reliability for intersegmental angle and displacement range, ICC,[2,12] was between 0.96 and 0.99 (Table 3). The SEM ranged from 0.4 to 0.7° and 0.57 to 0.89% displacement (0.2–0.3 mm based on a standard vertebral depth of 35 mm; Table 3).

Interimage Reliability. The average interimage reliability, ICC,[2,4] for minimum and maximum intersegmental angle was 0.91 (range, 0.82–0.94), and displacement was 0.84 (range, 0.64–0.93; Table 4). The SEM ranged from 0.7 to 1.4° and 1.2 to 2.1% displacement (0.4–0.7 mm based on a standard vertebral depth of 35 mm; Table 4). The average SEM across all segments was 1° and 0.6 mm (Table 4).

■ Discussion

The intraimage reliability values, ICC,[2,12] were all >0.96, were interpreted as good, and were greater than the 0.9 standard proposed[58] to ensure reasonable validity. The SEMs were minimal, 0.2 to 0.3 mm and 0.4 to 0.7° across segments. These error values were less than prior published error reports of 0.5 to 0.8 mm and 0.8 to 1.6° that used a similar measurement technique (Table

Table 4. Interimage ICC and SEM for the Current Study and Comparison with Frobin *et al*[40]

	Current Study			Frobin et al.[40]	
Segment	n*	ICC (2,12) †	SEM †	n ‡	SD
Midplane angle range (degrees)					
L3–L4	20	0.816–0.944	0.68 to 1.42°	54	0.85°
L4–L5	20	0.915–0.934	0.97 to 1.12°	52	1.32°
L5-S1	20	0.925–0.940	0.80 to 0.99°	11	1.64°
Average		0.913	1.00		
Intersegmental displacement range (mm)					
L3–L4	20	0.637–0.765	0.58 to 0.60 mm	54	0.52 mm
L4–L5	20	0.903–0.904	0.44 to 0.47 mm	52	0.55 mm
L5-S1	20	0.913–0.933	0.65 to 0.73 mm	11	0.84 mm
Average		0.842	0.58 mm		

* n = 20 images from 20 subjects during dynamic motion from upright to flexion
† ICC and SEM values for the current study represent the range of these reliability coefficients for the minimum and maximum values measured during the dynamic movement pattern.
‡ For L3–L4 and L4–L5: 6 cadaver specimens, 9 radiographs taken in different (0, +5, −5) degrees of rotation or tilt, for L5-S1:11 images of a bony phantom taken at different distances from the image intensifier.
‖ Example for intersegmental displacement was based on a vertebral depth of 35 mm (i.e., 0.6/35 mm = 0.017 or 1.7% relative displacement).

3).[40] Although the error measurements provided by Frobin *et al*[40] were obtained in vitro (therefore had less scatter of the DFV beam) with the specimen imaged at different orientations and were determined by different statistical techniques, the comparison reveals that the digital adaptation of the technique may have been better or at least comparable with their findings (Table 3). Therefore, the technique developed and used in this study was reliable, and repeated measures of the same DFV would be within 0.6 mm and 1.45° based on a 95% confidence interval (CI).

One of the closest comparisons possible to the work of Frobin *et al*[40] was with a step before the establishment of their error measurements. Frobin *et al*[40] provided the mean difference and the SD of the difference of intrarater assessment of images using the DCRA technique as assessed over repeated measurements (Table 5). The SD of the difference varied only 0.06% for displacement and 0.19° for angle evaluation, demonstrating only minimal differences between the static technique using hand-drawn then digitized vertebral body outlines from static radiographs used by Frobin *et al*[40] and the DFV technique.

As expected the interimage reliability coefficients decreased with the increased variability in human movement and patient positioning expected between analyses of images obtained from separate movement trials. The interimage reliability ICC^{2,4} values for midplane angle were all >0.82, and these were interpreted as good.[58] Further, five of the six midplane angle measurements tested were >0.9. The ICC^{2,4} values for displacement ranged from 0.64 to 0.93 and were interpreted as moderate to good,[58] with four of these six measurements being >0.9.

Table 5. Comparison of Intrareliability Data of the Current Study With the Results Published by Frobin *et al*[40]

	Current Study	Frobin *et al*[40]
No. of images	40 (2 sets of 20)	16 (1 set of 16)
No. of segments	120	78
Intersegmental midplane angle		
Mean Difference *	0.089°	0.015°
SD †	1.178°	0.992°
Intersegmental displacement		
Mean difference *	0.00083 (0.083%)	0.0005 (0.05%)
SD †	0.0154 (1.54%)	0.0148 (1.48%)

* Mean difference of the paired measurements from the segments.
† SD of the difference.

Although the ICC values at L3–L4 were lower than expected, the average 95% CI for the SEM across all segments remained low (<2° and 1.2 mm). The combination of the lower ICC values with acceptable SEM values highlights the mathematical limits and the paradox between these two measures of reliability.[59,60] Comparisons at the segmental level to the reported error values by Frobin *et al*[40] are provided in Table 4. The comparison reveals that the SEM at the 68% CI level measured in this study, relative to the SD reported by Frobin *et al*,[40] was comparable. Although there are differences in the methods in which these error measurements were obtained, the minimal differences between the two techniques support the claim by Frobin *et al*[40] in regard to the robustness of the DCRA technique.

Although this technique incorporated an automated computer algorithm to determine the corners of the vertebral body using a geometric principle of maximum distance, the algorithm was not designed to use an automatic vertebral body locator between the video frames. To make this technique useable in a clinical setting a more automated vertebral body location technique is required. Although prior attempts[26,61–63] at automatically locating the vertebral body have had some partial success, the use remains limited secondary to the continued technical restrictions. None of these previous techniques have tried to enhance the DFV before the application of an edge-detection technique. Future research should include use of an image enhancement technique.

In addition to automating the analysis, other types of additional technique-based and validity-based studies are required. This study used one repetition of movement as a

representation of the subject's motion pattern. An average of multiple movement trials (i.e., three repetitions) to represent the individual's motion pattern may be more representative of the true movement pattern, which potentially would improve the ICC and decrease the SEM, increasing the ability of this technique to assess significant kinematic changes over time. Further, analysis of the type of motion that should be measured needs to be determined. Previous researchers have used motion studies with the subject seated, standing, side lying, and/or a combination of positions with or without overpressure[6,21–23,47]; some have studied eccentric and concentric flexion,[43] as measured here, while others have measured the movement cycle from hyperextension to full flexion.[46] A comparison of how these movement patterns differ would allow for greater understanding in the interpretation of these different testing conditions. Additionally, the impact of different measurement techniques to determine intersegmental angle and displacement values[25,52] should be evaluated to determine the influence of their different approaches on the outcome measures. Further validating this technique with cadaveric models should be pursued.

In summary, the use of DCRA to measure the kinematic variables of the lumbar spine was a reliable technique with an average interimage SEM $< 2°$ and 1.2 mm (95% CI). The ability to enhance the images digitally before analysis appears to be a successful strategy that did not require the digitization of hand-drawn outlines of the vertebral bodies. Besides allowing direct measurement on the DFV images, this alteration allowed for greater automation of the process that ultimately allowed for the analysis of more frames per second (30 Hz) relative to prior videofluoroscopic studies (3–5 Hz).[44–46] To improve the ability to measure repeated movement over time, average measurements of multiple movement patterns may be more representative of the individual's movement pattern and therefore reduce the error associated with a test-retest design. Although the error measurements in this study were low, further improvement may be beneficial with regard to the ability of the responsiveness of this technique to detect change pre- and post-treatment (or surgery).

■ Key Points

- The use of distortion compensated roentgen analysis on digitally enhanced digital fluoroscopic video is a reliable method with acceptably low measurement error.
- The developed measurement technique provides a non invasive tool to assess dynamic lumbar movement patterns at 30 Hz.
- The technique has the potential to enhance understanding of the segmental and global kinematic movement patterns of those with lumbar segmental instability and the impact of surgical intervention on lumbar kinematics.

Acknowledgments

The authors thank Mr. Larry Wyatt and SPC Matthew Call for assistance and dedication to quality in the obtainment of the digital fluoroscopic videos.

References

1. Cherkin DC, Deyo RA, Loeser JD, et al. An international comparison of back surgery rates. *Spine* 1994;19:1201–6.
2. Waddell G. *The Back Pain Revolution*. First edition. New York: Churchill Livingstone, 1998.
3. Muggleton JM, Kondracki M, Allen R. Spinal fusion for lumbar instability: does it have a scientific basis? *J Spinal Disord* 2000;13:200–4.
4. Lund T, Oxland TR, Nydegger T, et al. Is there a connection between the clinical response after an external fixation test or a subsequent lumbar fusion and the pre-test intervertebral kinematics? *Spine* 2002;27:2726–33.
5. Posner I, White AA, 3rd, Edwards WT, et al. A biomechanical analysis of the clinical stability of the lumbar and lumbosacral spine. *Spine* 1982;7:374–89.
6. Dvorak J, Panjabi MM, Chang DG, et al. Functional radiographic diagnosis of the lumbar spine. Flexion-extension and lateral bending. *Spine* 1991;16:562–71.
7. Dupuis PR, Yong-Hing K, Cassidy JD, et al. Radiologic diagnosis of degenerative lumbar spinal instability. *Spine* 1985;10:262–76.
8. Ogon M, Bender BR, Hooper DM, et al. A dynamic approach to spinal instability. Part I: Sensitization of intersegmental motion profiles to motion direction and load condition by instability. *Spine* 1997;22:2841–58.
9. Nizard RS, Wybier M, Laredo JD. Radiologic assessment of lumbar intervertebral instability and degenerative spondylolisthesis. *Radiol Clin North Am* 2001;39:55–71, v-vi.
10. Hayes MA, Howard TC, Gruel CR, et al. Roentgenographic evaluation of lumbar spine flexion-extension in asymptomatic individuals. *Spine* 1989;14:327–31.
11. Tallroth K, Alaranta H, Soukka A. Lumbar mobility in asymptomatic individuals. *J Spinal Disord* 1992;5:481–4.
12. Sato H, Kikuchi S. The natural history of radiographic instability of the lumbar spine. *Spine* 1993;18:2075–9.
13. Tanz S. Motion of the lumbar spine. A roentgenologic study. *Am J Roentgenol Radium Ther Nucl Med* 1953;69:399–412.
14. Kirkaldy-Willis WH, Farfan HF. Instability of the lumbar spine. *Clin Orthop* 1982:110–23.
15. Deyo RA, McNiesh LM, Cone RO, 3rd. Observer variability in the interpretation of lumbar spine radiographs. *Arthritis Rheum* 1985;28:1066–70.
16. Putto E, Tallroth K. Extension-flexion radiographs for motion studies of the lumbar spine. A comparison of two methods. *Spine* 1990;15:107–10.
17. White APM. Clinical Biomechanics of the Spine. 2nd edition. Philadelphia, PA: JB Lippincott, 1990.
18. Steffen T, Rubin RK, Baramki HG, et al. A new technique for measuring lumbar segmental motion in vivo. Method, accuracy, and preliminary results. *Spine* 1997;22:156–66.
19. Lee SW, Wong KW, Chan MK, et al. Development and validation of a new technique for assessing lumbar spine motion. *Spine* 2002;27:E215–20.
20. Keessen W, During J, Beeker TW, et al. Recordings of the movement at the intervertebral segment L5–S1: a technique for the determination of the movement in the L5–S1 spinal segment by using three specified postural positions. *Spine* 1984;9:83–90.
21. Saraste H, Brostrom LA, Aparisi T, et al. Radiographic measurement of the lumbar spine. A clinical and experimental study in man. *Spine* 1985;10:236–41.
22. Wood KB, Popp CA, Transfeldt EE, et al. Radiographic evaluation of instability in spondylolisthesis. *Spine* 1994;19:1697–703.
23. Bronfort G, Jochumsen OH. The functional radiographic examination of patients with low-back pain: a study of different forms of variations. *J Manipulative Physiol Ther* 1984;7:89–97.
24. Knutsson F. The instability associated with disk degeneration in the lumbar spine. *Acta Radiol* 1944;25:593–609.
25. Shaffer WO, Spratt KF, Weinstein J, et al. 1990 Volvo Award in clinical sciences. The consistency and accuracy of roentgenograms for measuring sagittal translation in the lumbar vertebral motion segment. An experimental model. *Spine* 1990;15:741–50.
26. Muggleton JM, Allen R. Automatic location of vertebrae in digitized videofluoroscopic images of the lumbar spine. *Med Eng Phys* 1997;19:77–89.
27. Stokes IA, Frymoyer JW. Segmental motion and instability. *Spine* 1987;12:688–91.
28. Polly DW Jr, Kilkelly FX, McHale KA, et al. Measurement of lumbar lordosis. Evaluation of intraobserver, interobserver, and technique variability. *Spine* 1996;21:1530–5; discussion 5–6.

29. Penning L, Wilmink JT, van Woerden HH. Inability to prove instability. A critical appraisal of clinical-radiological flexion-extension studies in lumbar disc degeneration. *Diagn Imaging Clin Med* 1984;53:186–92.
30. Danielson B, Frennered K, Irstam L. Roentgenologic assessment of spondylolisthesis. I. A study of measurement variations. *Acta Radiol* 1988;29: 345–51.
31. Danielson B, Frennered K, Selvik G, et al. Roentgenologic assessment of spondylolisthesis. II. An evaluation of progression. *Acta Radiol* 1989;30: 65–8.
32. Boden SD, Wiesel SW. Lumbosacral segmental motion in normal individuals. Have we been measuring instability properly? *Spine* 1990;15:571–6.
33. Johnsson R, Selvik G, Stromqvist B, et al. Mobility of the lower lumbar spine after posterolateral fusion determined by roentgen stereophotogrammetric analysis. *Spine* 1990;15:347–50.
34. Lin RM, Yu CY, Chang ZJ, et al. Flexion-extension rhythm in the lumbosacral spine. *Spine* 1994;19:2204–9.
35. Pearcy M, Portek I, Shepherd J. Three-dimensional x-ray analysis of normal movement in the lumbar spine. *Spine* 1984;9:294–7.
36. Frobin W, Leivseth G, Biggemann M, et al. Vertebral height, disc height, posteroanterior displacement and dens-atlas gap in the cervical spine: precision measurement protocol and normal. *Clin Biomech (Bristol, Avon)* 2002; 17:423–31.
37. Frobin W, Leivseth G, Biggemann M, et al. Sagittal plane segmental motion of the cervical spine. A new precision measurement protocol and normal motion data of healthy adults. *Clin Biomech (Bristol, Avon)* 2002;17:21–31.
38. Leivseth G, Brinckmann P, Frobin W, et al. Assessment of sagittal plane segmental motion in the lumbar spine. A comparison between distortion-compensated and stereophotogrammetric roentgen analysis. *Spine* 1998;23: 2648–55.
39. Frobin W, Brinckmann P, Biggemann M, et al. Precision measurement of disc height, vertebral height and sagittal plane displacement from lateral radiographic views of the lumbar spine. *Clin Biomech (Bristol, Avon)* 1997; 12(Suppl 1):S1–63.
40. Frobin W, Brinckmann P, Leivseth G, et al. Precision measurement of segmental motion from flexion-extension radiographs of the lumbar spine. *Clin Biomech (Bristol, Avon)* 1996;11:457–65.
41. Brinckmann P, Frobin W, Biggemann M, et al. The shape of vertebrae and intervertebral discs - study of a young, healthy population and a middle-aged control group. *Clin Biomech (Bristol, Avon)* 1994;9:S1–83.
42. Rab G, Chao E. Verification of roentgenographic landmarks in the lumbar spine. *Spine* 1977;2:287–93.
43. Okawa A, Shinomiya K, Komori H, et al. Dynamic motion study of the whole lumbar spine by videofluoroscopy. *Spine* 1998;23:1743–9.
44. Kanayama M, Abumi K, Kaneda K, et al. Phase lag of the intersegmental motion in flexion-extension of the lumbar and lumbosacral spine. An in vivo study. *Spine* 1996;21:1416–22.
45. Kanayama M, Tadano S, Kaneda K, et al. A cineradiographic study on the lumbar disc deformation during flexion and extension of the trunk. *Clin Biomech (Bristol, Avon)* 1995;10:193–9.
46. Harada M, Abumi K, Ito M, et al. Cineradiographic motion analysis of normal lumbar spine during forward and backward flexion. *Spine* 2000;25: 1932–7.
47. Takayanagi K, Takahashi K, Yamagata M, et al. Using cineradiography for continuous dynamic-motion analysis of the lumbar spine. *Spine* 2001;26: 1858–65.
48. I-25, I-50, I-60, and I-75 [Foresight Imaging], 2002 [cited October 26, 2002]. Available from: www.foresightimaging.com.
49. *Image Pro-Plus* [computer program]. Version 4.5. Silver Spring, MD: Media Cybernetics, 2001.
50. *MATLAB* [computer program]. Version, Student Version 12. Natick, MA: MathWorks, 2001.
51. *SPSS Graduate Pack*. Version 11.0. Chicago, IL: SPSS Inc., 2001.
52. Muggleton JM, Allen R. Insights into the measurement of vertebral translation in the sagittal plane. *Med Eng Phys* 1998;20:21–32.
53. Harvey SB, Hukins DW. Measurement of lumbar spinal flexion-extension kinematics from lateral radiographs: simulation of the effects of out-of-plane movement and errors in reference point placement. *Med Eng Phys* 1998;20: 403–9.
54. Pearcy MJ. Stereo radiography of lumbar spine motion. *Acta Orthop Scand Suppl* 1985;212:1–45.
55. Image-Pro plus reference guide for windows. The proven solution for image analysis. Silver Spring, MD: Media Cybernetics, 2001.
56. Bovik A, editor. *Handbook of Image and Video Processing*. First edition. San Diego, CA: Academic Press, 2000.
57. Cholewicki J, McGill S, Wells R, et al. Method for measuring vertebral kinematics from videofluoroscopy. *Clin Biomech (Bristol, Avon)* 1991;6: 73–8.
58. Portney L, Watkins M. Foundations of clinical research: applications to practice. First edition. Norwalk, CT: Appleton & Lange, 1993.
59. Wainner RS. Reliability of the clinical examination: how close is "close enough"? *J Orthop Sports Phys Ther* 2003;33:488–91.
60. Russek L. Factors affecting interpretation of reliability coefficients. *J Orthop Sports Phys Ther* 2004;34:341–9.
61. Breen AC, Allen R, Morris A. Spine kinematics: a digital videofluoroscopic technique. *J Biomed Eng* 1989;11:224–8.
62. Breen A, Allen R, Morris A. A digital videofluoroscopic technique for spine kinematics. *J Med Eng Technol* 1989;13:109–13.
63. Zheng Y, Nixon MS, Allen R. Lumbar spine visualisation based on kinematic analysis from videofluoroscopic imaging. *Med Eng Phys* 2003;25: 171–9.